leading to values of $\varphi_0$ and $\delta$ for the O–O lines shown in Table 3.

Table 3. *Orientations of the* O–O *lines which involve acceptor oxygen atoms different from those suggested in the X-ray work*

| H-bonding scheme | $\varphi$ | $\delta$ |
|---|---|---|
| $O_1$–$(H_2O)_2$–$tO_1$ | 26° | 23° |
| $tO_1$–$(H_2O)_3$–$O_3$ | 150 | 45 |

Though these values are in better agreement with the experimental values for (p–p)II and (p–p)III, shown in Table 1, the distances $(H_2O)_2$–$O_1$ and $(H_2O)_3$–$O_3$ are rather too large, being about 4 Å.

The angles O–$H_2O$–O are in the range between 108° and 112° for all the bonding schemes considered here and so this does not provide us with a basis for making a choice.

## Conclusions

If the hydrogen bonding scheme suggested by Broomhead & Nicol (1948) is assumed to be correct, we find that the parallelism between the p–p and the O–O lines usually found in hydrates is not present here, even though the bond lengths are normal. Alternatively the hydrogen bonding schemes suggested by them are not the right ones and we have to look for other acceptors in the structure.

The only other set of acceptor atoms we could find is such that the bond lengths are too large, even though the parallelism between the p–p and the O–O lines is fairly reasonable.

The difficulty encountered in fixing the hydrogen bonding schemes is probably a result of the fact that the accuracy of the X-ray work is rather poor. We feel that a refinement of the structure will help to fix the hydrogen-bonded atoms and hence the proton positions.

We are deeply indebted to Professor R. S. Krishnan for his kind interest and to Professor P. S. Narayanan for supplying the infrared results.

## References

BROOMHEAD, J. M. & NICOL, A. D. I. (1948). *Acta Cryst.* **1**, 88.
PAKE, G. E. (1948). *J. Chem. Phys.* **16**, 237.

*Acta Cryst.* (1969). B**25**, 1503

# The Albite Structures

BY P. H. RIBBE*, HELEN D. MEGAW AND W. H. TAYLOR
*Crystallographic Laboratory, Cavendish Laboratory, Cambridge, England*

[AN ANALYSIS BASED ON EXPERIMENTAL MEASUREMENTS
BY R. B. FERGUSON
*Department of Geology, University of Manitoba, Winnipeg, Canada*
AND R. J. TRAILL
*Geological Survey of Canada, Ottawa, Canada*]

(*Received* 6 *May* 1968)

Three-dimensional analyses of the low albite and high albite studied by Ferguson, Traill & Taylor in 1958 have confirmed that in the low temperature material the Al,Si distribution is highly ordered, in the high temperature almost completely random, and have also confirmed the marked anisotropy of the Na atom in both materials. The improved accuracy has shown that in low albite the sites $T_1(m)$, $T_2(0)$, $T_2(m)$ are almost free of Al, whereas the earlier analysis required the allocation of a small amount of Al to $T_2(0)$. The observed anisotropy of the Na atom in low albite may be interpreted in terms of a multipartite structure with faulted domains, though an explanation in terms of anisotropic thermal vibration is more probable. For high albite the very large anisotropy of the Na atom, and the diffuse nature of the atomic peaks of electron density, point to the interpretation of the diffraction pattern as representing only an average structure; in this material the evidence for a multipartite structure with faulted domains is considerably stronger than for low albite.

An Appendix compares the effects of temperature factor with those of 'splitting' of atoms.

## 1. Introduction

The first examination of the structure of (low) albite, $NaAlSi_3O_8$ (Taylor, Darbyshire & Strunz, 1934), which established its relationship to other felspar structures, was followed in 1958 by two-dimensional analyses of low albite and high albite by Ferguson, Traill & Taylor. These analyses showed that in low albite the Al,Si distribution is highly ordered whereas in high albite it is random or very nearly so. They also revealed the markedly anisotropic character of the Na atom, which

* Present address: Department of Geological Sciences, Virginia Polytechnic Institute, Blacksburg, Virginia, U.S.A.

is very elongated in both structures. The present paper describes full three-dimensional analyses of the low and high albites studied by Ferguson *et al.* and discusses the structures thus determined in terms of concepts gradually evolved from the study of felspar structures in the last few years. A preliminary account of the refinement of the low albite structure was published by Ribbe, Ferguson & Taylor (1962), and much of the work on both structures was described in a thesis by Ribbe (1963) and in a paper presented at a meeting of the Geological Society of America (Ribbe, Ferguson, Traill & Taylor, 1963). A detailed comparison of low albite with reedmergnerite was given by Appleman & Clark (1965).

Two major features of the structures dominate the interpretation of the structural details of both low and high forms of albite: first the Al, Si distribution in the framework of linked tetrahedra, and secondly the anisotropy of the Na atom.

(i) The size of a tetrahedral group in a felspar (defined as the average T–O distance where T is Al or Si) is slightly larger for $AlO_4$ than for $SiO_4$; where the measured size lies between these extremes, it must represent an average of groups some containing Al, others Si. The relationship between tetrahedron size and Al, Si occupancy is not uniquely determined from independent measurements, but rests upon the whole set of felspar measurements, and as more accurate measurements have become available the earlier relation proposed by Smith (1954) has been modified by Smith & Bailey (1963). (See also Ribbe & Gibbs, 1967; Jones, 1968).

In this way tetrahedron size measurements are first translated into fractional Al, Si occupancies and it remains to devise a physically meaningful interpretation of these occupancies throughout the structure. Two models which will be considered in some detail for albite are the straightforward space average on the unit-cell scale, and a texture in which a fixed and regular distribution repeats throughout each small domain, the observed average being produced by stacking faults between domains.

(ii) The observed anisotropy of the Na atom in both low albite and high albite receives its simplest interpretation as the time-average of a true anisotropic thermal vibration of the atom within the cavity formed by the surrounding O atoms, but from the first (Ferguson *et al.* 1958) it has seemed quite unrealistic to attempt to explain the very large anisotropy in high albite in this way. Alternatively, in different unit cells chosen at random the Na atom may be located at different points within the same cavity, in which case the 'elongated' atom represents a simple space average. A third possibility is that the space average is a consequence of the random faulting of a perfectly regular structure with a larger unit cell, in which a limited number of different sites are occupied in a repetitive way within a domain, but the domains are small and bounded by randomly occurring faults. In an attempt to decide between the interpretation as a time average and that in terms of some kind of space average, both low albite and high albite were examined (by two-dimensional methods) at −180 °C (Williams, 1961; Williams & Megaw, 1964). The results, not entirely conclusive, favour a space average; they are considered, below, in relation to the accurate structure analyses at room temperature now reported.

Sections 2 and 4 contain outline accounts of the procedures followed in the refinement of low albite and high albite structures, and details of the structures as finally determined. Full information on both experimental measurements and methods of interpretation used in the structure analyses is available in a thesis (Ribbe, 1963). Detailed information about the materials used (low albite from Ramona, high albite prepared by heating low albite from Amelia, Virginia) is given by Ferguson *et al.* (1958).

Discussions of the low albite structure (§ 3) and the high albite structure (§ 5) are followed by brief reference to certain outstanding problems of the albite structures.

A comparison of the effects of temperature factor and 'splitting' of atoms is given in an Appendix.

## 2. Refinement of the low albite structure

At the time when the two-dimensional refinements of the albite structures were carried out (Ferguson *et al.*

Table 1. *Low albite. Scattering factors for refinement stages* (i) (ii) *and* (iii)

Coefficients in the expression* $A \exp(-\frac{1}{4}as^2) + B \exp(-\frac{1}{4}bs^2) + C$ where $s = 2 \sin\theta/\lambda$.

| | $A$ | $a$ | $B$ | $b$ | $C$ | Reference |
|---|---|---|---|---|---|---|
| $Na^+$ | 7·471 | 4·007 | 0·874 | 131·13 | 1·623 | Derived from data in Berghuis *et al.* (1955), using the method of Forsyth & Wells (1959) |
| $O^{2-}$ | 4·455 | 5·891 | 4·225 | 44·57 | 1·355 | |
| $Al^{3+}$ | 5·151 | 1·806 | 3·402 | 5·087 | 1·442 | Forsyth & Wells (1959) on data from Froese (1957) |
| $Si^{4+}$ | 5·138 | 1·459 | 3·442 | 3·982 | 1·420 | Forsyth & Wells (1959) on data from Berghuis *et al.* (1955) |
| $\frac{1}{4}Al^{3+} + \frac{3}{4}Si^{4+}$ | 4·952 | 1·477 | 3·643 | 4·151 | 1·402 | Weighted curve using the method of Forsyth & Wells (1959) on data from Berghuis *et al.* (1955) and Froese (1957) |

* The expression quoted differs from that of Forsyth & Wells (1959) by a factor of $\frac{1}{4}$ in each exponential term as a consequence of the use of $s = 2 \sin\theta/\lambda$, whereas the '$s$' used by Forsyth & Wells is defined as $\sin\theta/\lambda$.

1958) the intensities needed for a complete three-dimensional refinement of the low albite structure were measured visually by Ferguson, using multiple film techniques, corrected for Lorentz and polarization effects, and put on an absolute scale after completion of the two-dimensional refinement. Absorption effects were negligible; no effects attributable to extinction were observed. Altogether, 1994 observed $F(hkl)$ values were available for the refinement now reported.

The refinement process was in four well-defined stages. The first three used a difference-Fourier program (with the computer EDSAC II in the Cambridge University Mathematical Laboratory) which selected the best atomic coordinates and the best isotropic temperature factor for each atom. Atomic scattering factors were obtained by the method of Forsyth & Wells (1959), assuming full ionization for all atoms and using the constants listed in Table 1. The fourth stage, a full-matrix least-squares refinement using a modified version of the program of Busing, Martin & Levy (1962), was carried out in the University of Chicago with the help of Mr C. R. Knowles. In the least-squares refinement the atomic scattering factors of Na, Al, Si and O were taken from Vol. III of *International Tables for X-ray Crystallography* modified for half-ionized atoms and averaged over ($\frac{1}{4}$ Al + $\frac{3}{4}$ Si). The final parameters are listed in Table 2 and their errors in Table 3.

(i) Starting with the atomic positions given by Ferguson *et al.* (1958), with the same scattering factor curve ($\frac{1}{4} f_{Al} + \frac{3}{4} f_{Si}$) for all atoms $T$ (=Al or Si), and

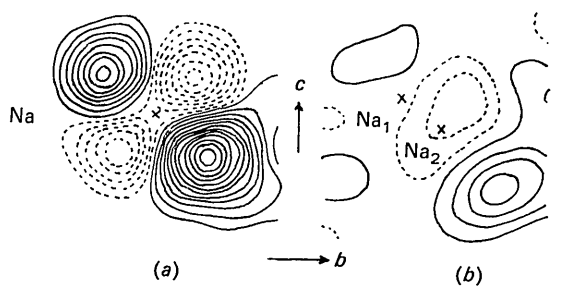


Fig. 1. Low albite. The anisotropy of the sodium atom shown in difference sections ($\varrho_o - \varrho_c$) parallel to (100) and passing through the centres of the atoms. (*a*) End of stage (i) of refinement, $R$ 0·101, $B_{Na}$ (isotropic) 2·35 Å$^2$. (*b*) End of stage (ii) of refinement $R$ 0·092, $B_{\frac{1}{2}Na}$ (isotropic) 1·42 Å$^2$. Positive contours full line, negative dotted, zero contour omitted. Contour interval 0·165 e.Å$^{-3}$. The vector connecting half-atoms $Na_1$ and $Na_2$ lies very nearly in the (100) plane [see text and Table 2(*b*)].

Table 2. *Low albite*

(*a*) Final atomic coordinates, in fractions of the cell edge

| | $x$ | $y$ | $z$ |
|---|---|---|---|
| Na | 0·2682 | 0·9888 | 0·1462 |
| $T_1(0)$ | 0·0088 | 0·1692 | 0·2081 |
| $T_1(m)$ | 0·0041 | 0·8202 | 0·2375 |
| $T_2(0)$ | 0·6919 | 0·1102 | 0·3148 |
| $T_2(m)$ | 0·6813 | 0·8820 | 0·3604 |
| $O_A(1)$ | 0·0055 | 0·1308 | 0·9664 |
| $O_A(2)$ | 0·5929 | 0·9974 | 0·2808 |
| $O_B(0)$ | 0·8124 | 0·1101 | 0·1905 |
| $O_B(m)$ | 0·8200 | 0·8512 | 0·2587 |
| $O_C(0)$ | 0·0132 | 0·3035 | 0·2690 |
| $O_C(m)$ | 0·0239 | 0·6935 | 0·2291 |
| $O_D(0)$ | 0·2075 | 0·1091 | 0·3890 |
| $O_D(m)$ | 0·1840 | 0·8681 | 0·4348 |

(*b*) Half-atom coordinates of Na, at the end of stage (ii)

| | $x$ | $y$ | $z$ |
|---|---|---|---|
| $Na_1$ | 0·2723 | 0·9776 | 0·1627 |
| $Na_2$ | 0·2650 | 0·9995 | 0·1300 |

with (isotropic) temperature factors $B_{Na}$ 1·65 Å$^2$, $B_T$ 0·6 Å$^2$ and $B_O$ 1·25 Å$^2$, the $R$ index was gradually reduced from 0·149 to 0·101. This was achieved by the introduction of small shifts in the atomic coordinates and of improved temperature factors, and by assigning the scattering factor curves $f_{Al}$ or $f_{Si}$ (instead of the average $\frac{1}{4} f_{Al} + \frac{3}{4} f_{Si}$) to the appropriate atoms as the nature of the ordered distribution became increasingly clear with the progress of the refinement. At the end of this stage a difference section ($\varrho_o - \varrho_c$) parallel to (100) and passing through the centre of the Na atom [Fig. 1(*a*)] displayed the anisotropy of the atom very strikingly. The (isotropic) temperature factor assumed for Na was now 2·35 Å$^2$.

(ii) The marked anisotropy of the Na atom was next taken into account by refining a structure model in which the single Na atom is replaced by two half-atoms, each with its own isotropic temperature factor, separated by a suitable distance along the direction of the major axis of the ellipsoidal (anisotropic) single atom. This familiar 'split-atom' approximation, already used by Williams (1961) in his study of albite, and discussed briefly in the Appendix to this paper, resulted in further improvement in the difference density ($\varrho_o - \varrho_c$) and a corresponding reduction in the $R$ index. This stage of the refinement introduced only very small changes in the positions and isotropic temperature factors for T and O atoms, and was completed with $R$ = 0·092. Atomic

Table 3. *Low albite. Average coordinate errors*

| | Average error in coordinates* | | | Maximum error in position† |
|---|---|---|---|---|
| | $\sigma(x)$ | $\sigma(y)$ | $\sigma(z)$ | |
| Na | 0·0004 | 0·0003 | 0·0005 | 0·0038 Å |
| T | 0·0002 | 0·0001 | 0·0002 | 0·0016 |
| O | 0·0005 | 0·0003 | 0·0006 | 0·0043 |

* For atoms T and O the error quoted is the *average* for each coordinate.
† Error in atomic position is the maximum value $\sigma(x)a$, $\sigma(y)b$, or $\sigma(z)c$.

coordinates thus determined for the half-atoms $Na_1Na_2$ are quoted in Table 2(*b*); other atomic coordinates are not listed. Temperature factors for all atoms except the half-atoms $Na_1Na_2$ are quoted in Table 4. For $Na_1Na_2$ the temperature factor $B_{1/2Na}$ is 1·42 Å², the distance between half-atoms is 0·364 Å, and the vector connecting $Na_1$ and $Na_2$ lies almost exactly in the (100) plane. The half-separation, 0·182 Å, is too small to give rise to any significant differences in intensities calculated from the split-atom model and the anisotropic-atom model (see Appendix). In Fig. 1(*b*) a difference section ($\varrho_o - \varrho_c$) parallel to (100) and passing through the half-atoms $Na_1$, $Na_2$ may be compared with Fig. 1(*a*); it is clear that the split-atom model provides a good, though not perfect, representation of the anisotropic Na atom.

(iii) The possibility that the use of half-atoms to represent the Na atom anisotropy might be unduly restrictive was tested by examining a model comprising four quarter-atoms. Attempts to refine this model led to no important improvement by comparison with the half-atom model. The analysis in the Appendix would suggest that none was to be expected, since even the half-atom model is only at the limit of resolution. The quarter-atom model was discarded.

(iv) A least-squares refinement was used as the final stage. For this program half-ionized atoms averaged over $\frac{1}{4}Al+\frac{3}{4}Si$ were assumed, as opposed to fully-ionized atoms identified as Al and Si in the difference-Fourier refinement procedure for (i) to (iii) above. The Na atom was taken as a normal single atom, not as two half-atoms. In stage iv(*a*) two cycles of refinement of atomic coordinates and isotropic temperature factors reduced $R$ from 0·092 to 0·087, but a marked improvement to $R=0{\cdot}068$ resulted from the introduction of anisotropic temperature factors for all atoms in a further three cycles [stage iv(*b*)] in which atomic positional coordinates were also very slightly modified.

The structure described by these final atomic coordinates and anisotropic temperature factors is comparable in accuracy with other felspar structures recently refined by three-dimensional methods, and thus supersedes the analysis of Ferguson *et al.* (1958) and the room-temperature analysis of Williams (1961), as well as the published preliminary account of the present work (Ribbe *et al.* 1962). Details of the atomic coordinates, thermal parameters, interatomic distances and interbond angles in the structure, and their errors, are given in Tables 2 to 8. In considering the tabulated information the following points should be noted:

(*a*) Of the final atomic coordinates listed in Table 2, those for atoms T are almost identical with the coordinates obtained from stage (ii) of the refinement, two of those for atoms O [$z$ for $O_A(2)$ and $x$ for $O_C(0)$] differ from stage (ii) values by 0·0010, and $z$ for Na differs by 0·0013. Correspondingly, in Tables 5 and 6 the mean T–O and O–O distances differ by negligible amounts from those obtained at the end of stage (ii) which were $T_1(0)$ 1·744 and 2·844 Å, $T_1(m)$ 1·611 and 2·629 Å, $T_2(0)$ 1·614 and 2·636 Å, $T_2(m)$ 1·613 and 2·631 Å. Similarly for the interbond angles of Table 7 the differences on comparison with stage (ii) are mostly very small and never exceed 0·5°.

Table 4. *Low albite. Thermal parameters*

| | Isotropic temperature factors (Å²) | | Anisotropic thermal parameters [Stage (iv(*b*))]† | | | | | | | | |
|---|---|---|---|---|---|---|---|---|---|---|---|
| | Stages (i), (ii)* | Stage iv(*a*)† | $b_{11}$ | $b_{22}$ | $b_{33}$ | $b_{12}$ | $b_{13}$ | $b_{23}$ | $B_{max}$ | $B_{int}$ | $B_{min}$ |
| | | | $\times 10^{-4}$ | | | | | | (Å²) | | |
| Na | 2·35 | 2·40 | 59 | 55 | 158 | −12 | 37 | −53 | 5·4 | 1·4 | 1·1 |
| $T_1(0)$ | 0·62 | 0·81 | 44 | 12 | 46 | −5 | 20 | 4 | 1·1 | 0·8 | 0·6 |
| $T_1(m)$ | 0·60 | 0·45 | 31 | 6 | 26 | 0 | 14 | 5 | 0·7 | 0·5 | 0·2 |
| $T_2(0)$ | 0·65 | 0·54 | 27 | 6 | 37 | −1 | 10 | 4 | 0·8 | 0·5 | 0·3 |
| $T_2(m)$ | 0·61 | 0·51 | 25 | 5 | 38 | 0 | 12 | 4 | 0·7 | 0·5 | 0·3 |
| $O_A(1)$ | 1·03 | 1·01 | 69 | 17 | 43 | 2 | 28 | 5 | 1·5 | 1·1 | 0·6 |
| $O_A(2)$ | 0·90 | 0·78 | 35 | 8 | 64 | −3 | 14 | 11 | 1·4 | 0·7 | 0·3 |
| $O_B(0)$ | 1·05 | 1·15 | 65 | 16 | 83 | −10 | 46 | −2 | 1·7 | 1·1 | 0·7 |
| $O_B(m)$ | 1·19 | 1·38 | 69 | 18 | 115 | 5 | 60 | 2 | 2·0 | 1·3 | 0·8 |
| $O_C(0)$ | 1·00 | 1·02 | 41 | 15 | 75 | −9 | 29 | −10 | 1·6 | 0·9 | 0·6 |
| $O_C(m)$ | 1·02 | 1·07 | 41 | 15 | 63 | −1 | 4 | 6 | 1·6 | 1·0 | 0·7 |
| $O_D(0)$ | 1·11 | 1·17 | 61 | 17 | 56 | 7 | 15 | 9 | 1·6 | 1·2 | 0·7 |
| $O_D(m)$ | 1·16 | 1·37 | 64 | 17 | 71 | −11 | 9 | −5 | 2·0 | 1·4 | 0·7 |

* Scattering factor curve for $T_1(0)\ldots f_{Al^{3+}}$; for $T_1(m)$, $T_2(0)$, $T_2(m)\ldots f_{Si^{4+}}$; fully-ionized atoms.

† Average $f$ curve for all half-ionized T atoms ($\frac{1}{4}f_{Al}+\frac{3}{4}f_{Si}$).

Standard errors: for isotropic temperature factors Na 0·06, T 0·02, O 0·06 Å²; for anisotropic thermal parameters $b$ Na 4, T 2, O 4 ($\times 10^{-4}$).

Anisotropic 'temperature factors' $B_{max}$ $B_{int}$ $B_{min}$ (along axes $r_3$ $r_2$ $r_1$) correspond to the anisotropic thermal parameters $b_{11}\ldots b_{23}$ for each atom.

For the Na atom the 'temperature factors' correspond to a 'vibration' ellipsoid with r.m.s. components of 'thermal' displacement 0·261, 0·133, 0·118 Å (average error 0·005 Å); the major axis is inclined at the angles 78°, 37°, 131°, (average error 1°) to the crystallographic axes $a,b,c$. [Further details of the orientations of the ellipsoids may be obtained on application to P.H. Ribbe.]

Table 5. *Low albite.* T–O *bond lengths* (Å)

| | | Mean | | | Mean |
|---|---|---|---|---|---|
| $T_1(0)$ –$O_A(1)$ | 1·750 | | $T_2(0)$ –$O_A(2)$ | 1·629 | |
| –$O_B(0)$ | 1·746 | 1·746 | –$O_B(0)$ | 1·592 | 1·615 |
| –$O_C(0)$ | 1·738 | | –$O_C(m)$ | 1·615 | |
| –$O_D(0)$ | 1·749 | | –$O_D(m)$ | 1·623 | |
| $T_1(m)$–$O_A(1)$ | 1·601 | | $T_2(m)$–$O_A(2)$ | 1·641 | |
| –$O_B(m)$ | 1·603 | 1·610 | –$O_B(m)$ | 1·617 | 1·612 |
| –$O_C(m)$ | 1·622 | | –$O_C(0)$ | 1·587 | |
| –$O_D(m)$ | 1·615 | | –$O_D(0)$ | 1·604 | |

Average standard error in T–O bond lengths is $0{\cdot}004_6$ Å.
Standard error in mean T–O bond lengths is $0{\cdot}002_3$ Å.

Table 6. *Low albite.* O–O *interatomic distances* (Å)

| Tetrahedron | $O_A-O_B$ | $O_A-O_C$ | $O_A-O_D$ | $O_B-O_C$ | $O_B-O_D$ | $O_C-O_D$ | Tetrahedral mean |
|---|---|---|---|---|---|---|---|
| $T_1(0)$ | 2·731 | 2·956 | 2·751 | 2·899 | 2·876 | 2·865 | 2·846 |
| $T_1(m)$ | 2·607 | 2·683 | 2·582 | 2·616 | 2·661 | 2·623 | 2·630 |
| $T_2(0)$ | 2·659 | 2·565 | 2·611 | 2·656 | 2·662 | 2·660 | 2·636 |
| $T_2(m)$ | 2·621 | 2·572 | 2·636 | 2·629 | 2·639 | 2·688 | 2·631 |
| Bond mean | 2·655 | 2·694 | 2·645 | 2·700 | 2·710 | 2·709 | |

Average standard error in O–O bond lengths is $0{\cdot}006_1$ Å.
Standard error in tetrahedral mean bond lengths is $0{\cdot}002_5$ Å.

Table 7. *Low albite. Interbond angles, in degrees*

T–O–T angles

| | |
|---|---|
| $T_1(0)$ –$O_A(1)$ –$T_1(m)$ | 140·7 |
| $T_2(0)$ –$O_A(2)$ –$T_2(m)$ | 130·5 |
| $T_1(0)$ –$O_B(0)$ –$T_2(0)$ | 139·6 |
| $T_1(m)$–$O_B(m)$–$T_2(m)$ | 161·2 |
| $T_1(0)$ –$O_C(0)$ –$T_2(m)$ | 129·6 |
| $T_1(m)$–$O_C(m)$–$T_2(0)$ | 135·7 |
| $T_1(0)$ –$O_D(0)$ –$T_2(m)$ | 134·0 |
| $T_1(m)$–$O_D(m)$–$T_2(0)$ | 151·2 |
| Mean | 140·3 |

O–T–O angles

| | | | | | |
|---|---|---|---|---|---|
| $O_A(1)$–$T_1(0)$ | –$O_B(0)$ | 102·8 | $O_A(2)$–$T_2(0)$ | –$O_B(0)$ | 111·3 |
| | –$O_C(0)$ | 115·9 | | –$O_C(m)$ | 104·5 |
| | –$O_D(0)$ | 103·7 | | –$O_D(m)$ | 106·8 |
| $O_B(0)$– | –$O_C(0)$ | 112·6 | $O_B(0)$– | –$O_C(m)$ | 111·8 |
| | –$O_D(0)$ | 110·8 | | –$O_D(m)$ | 111·8 |
| $O_C(0)$– | –$O_D(0)$ | 110·5 | $O_C(m)$– | –$O_D(m)$ | 110·4 |
| $O_A(1)$–$T_1(m)$– | $O_B(m)$ | 108·9 | $O_A(2)$–$T_2(m)$– | $O_B(m)$ | 107·1 |
| | –$O_C(m)$ | 112·8 | | –$O_C(0)$ | 105·8 |
| | –$O_D(m)$ | 106·8 | | –$O_D(0)$ | 108·6 |
| $O_B(m)$– | –$O_C(m)$ | 108·5 | $O_B(m)$– | –$O_C(0)$ | 110·3 |
| | –$O_D(m)$ | 111·6 | | –$O_D(0)$ | 110·0 |
| $O_C(m)$– | –$O_D(m)$ | 108·3 | $O_C(0)$– | –$O_D(0)$ | 114·7 |

Mean tetrahedral angle 109·4°

Standard error of all bond angles is 0·2°.

Table 8. *Low albite.* Na–O *interatomic distances* (Å)

| Oxygen | Na(0000) | $Na_1$(half-atom) | $Na_2$(half-atom) |
|---|---|---|---|
| $O_A(1000)$ | 2·66 | 2·80 | 2·54 |
| $O_A(100c)$ | 2·54 | 2·46 | 2·62 |
| $O_A(2000)$ | 2·38 | 2·37 | 2·38 |
| $O_A(200c)$ | 3·72 | 3·62 | 3·84 |
| $O_A(200c)$ | 3·73 | 3·83 | 3·61 |
| $O_B(000c)$ | 2·46 | 2·49 | 2·43 |
| $O_B(m00c)$ | 3·47 | 3·64 | 3·29 |
| $O_C(0zi0)$ | 2·95 | 2·83 | 3·09 |
| $O_C(mzi0)$ | 3·26 | 3·38 | 3·15 |
| $O_D(0000)$ | 2·44 | 2·45 | 2·44 |
| $O_D(m000)$ | 2·99 | 2·83 | 3·16 |

Shortest Na–Na distance 3·92

All distances are rounded off to two decimal places. Distances Na–O are calculated from the final atomic coordinates of Table 2(*a*). Distances $Na_1$–O and $Na_2$–O are calculated from the sodium half-atom coordinates at the end of stage (ii) of the refinement as in Table 2(*b*). The oxygen atom coordinates used are also those obtained at the end of stage (ii) which differ only very slightly from those listed in Table 2(*a*) (see text).

Average standard error in Na–O bond lengths is $0{\cdot}005_7$ Å.

(*b*) Table 4 collects the thermal parameters for all atoms at various stages in the refinement process. Two sets of isotropic temperature factors are quoted, both retaining the single Na atom; the first (assuming fully-ionized atoms) takes account of the ordering of Al into the site $T_1(0)$, the second (assuming half-ionized atoms) ignores the ordering of Al. The temperature factor found for a given atom clearly depends in part on the scattering curve selected for the atom; in this respect the results of stage (ii) are preferable to those of stage (iv) for the T atoms. The anisotropic temperature factors are conveniently considered in terms of the ellipsoid with axes $B_{\max}$ $B_{\text{int}}$ $B_{\min}$; for the Na atom the corresponding (r.m.s.) amplitudes of thermal vibration are shown at the foot of the Table. The angles between the axes of the vibration ellipsoid for Na and the crystal axes *a b c* are quoted; the direction of the principal axis may be compared with the almost identical direction found in refinement stage (ii) [Table 2 (*b*)] and defined by angles 81°, 36°, 129°, to *a b c* axes.

The half-atom separation corresponding to the vibration ellipsoid of the Na atom (Table 4) is given by $2d$ where $8\pi^2d^2 \times 1{\cdot}44 = B_{max} - B_{int}$ (see Appendix), whence $2d = 0{\cdot}374$ Å; the directly determined value in refinement stage (ii), with $B_{1/2Na}$ 1·42 Å$^2$, was 0·364 Å.

In comparison with the anisotropy of the Na atom, the anisotropies of the T atoms are less important. Their nature (as seen in difference Fourier sections in the course of the refinement of the structure) suggests the possibility of either systematic error or interaction with the Na anisotropy, and they will not be discussed further. [See also § 4 (iii) below].

### 3. Discussion of the low albite structure

The following discussion is based on the description of the analysis of the structure in § 2, and on the details given in Tables 2 to 8.

(i) *The* Al, Si *distribution*

The mean tetrahedron sizes (Table 5) are collected in Table 9, with the corresponding Al contents deduced from the relationship of Smith & Bailey (1963). Application of the Cruickshank (1949) test for significance confirms expectation that the differences between the size of the ideal $SiO_4$ tetrahedron and the observed tetrahedron sizes for $T_1(m)$, $T_2(0)$ and $T_2(m)$ are not significant. Moreover, these three tetrahedra differ only to an extent which is statistically non-significant from the corresponding tetrahedra in reedmergnerite, the boron analogue of low albite (Appleman & Clark, 1965; see also Clark & Appleman, 1960); since Al in albite is replaced in reedmergnerite by B which is *smaller* than Si, the conclusion is that both structures are highly ordered, with all the Al of $NaAlSi_3O_8$ in tetrahedron $T_1(0)$.

The figures for tetrahedron sizes obtained by Ferguson *et al.* (1958) are also listed in Table 9. The present three-dimensional study is more reliable than their two-dimensional analysis, and it is clear that their sizes for $T_1(m)$ and $T_2(0)$ are inaccurate. The corresponding Al contents derived from the Smith & Bailey (1963) relationship (Table 9) necessarily show the same trend as the Al contents deduced by Ferguson *et al.* from Smith's (1954) curve and in particular a significant amount of Al is placed in the site $T_2(0)$. Ferguson *et al.* proposed, with this Al distribution as the starting point, that the stability of a felspar structure might be determined by the local balance of charge or electrostatic valency; since the three-dimensional structure analysis does not confirm this allocation of Al to site $T_2(0)$, but places all the Al of low albite in the site $T_1(0)$, the basis for the charge-balance hypothesis is proved false (see also Brown & Bailey, 1964).

A comparison of the temperature factors determined for the T atoms (Table 4) with those found for highly ordered microclines emphasizes the close inter-relationship between temperature factor and the atomic scattering curve assumed in the analysis. Table 10 shows that isotropic temperature factors are nearly the same for all T atoms in the structure when the scattering curve for Al is allocated to $T_1(0)$ and the scattering curve for Si to $T_1(m)$, $T_2(0)$, $T_2(m)$, whereas the temperature

Table 9. *Low albite.* Al, Si *distribution*

| | (1) This investigation | | (2) Ferguson *et al.* (1958) | |
|---|---|---|---|---|
| Tetrahedron | Mean T–O distance | Al content | Mean T–O distance | Al content |
| $T_1(0)$ | 1·746 Å | 0·97 | 1·742 Å | 0·95 |
| $T_1(m)$ | 1·610 | 0·00 | 1·590 | 0 |
| $T_2(0)$ | 1·615 | 0·03 | 1·636 | 0·19 |
| $T_2(m)$ | 1·612 | 0·02 | 1·616 | 0·04 |
| | Total Al | 1·02 | Total Al | 1·18 |

*Note*: Al contents are deduced in *both* cases from the relationship of Smith & Bailey (1963). See also Ribbe & Gibbs (1967) and Jones (1968).

Table 10. *Isotropic temperature factors for* T *atoms in highly ordered structures*

| | Low albite (see Table 4) | | Authigenic microcline (Finney & Bailey, 1964) | | Igneous microcline (Brown & Bailey, 1964) | |
|---|---|---|---|---|---|---|
| Tetrahedron | (1) | (2) | (1) | (2)* | (1) | (2) |
| $T_1(0)$ | 0·62 | 0·81 | 0·60 | | 0·29 | 0·69 |
| $T_1(m)$ | 0·60 | 0·45 | 0·61 | | 0·38 | 0·35 |
| $T_2(0)$ | 0·65 | 0·54 | 0·56 | | 0·38 | 0·34 |
| $T_2(m)$ | 0·61 | 0·51 | 0·54 | | 0·35 | 0·31 |

Column (1) for each material refers to calculations based on scattering curves $T_1(0) = Al$; $T_1(m)$, $T_2(0)$, $T_2(m) = Si$; column (2) corresponds to an average scattering curve ($\frac{1}{4}Al + \frac{3}{4}Si$) for all atoms. Different degrees of ionization are assumed in different calculations; the comparisons between columns (1) and (2) are modified only slightly as a consequence.

* For the authigenic microcline the figures for column (2) are not available, but Finney & Bailey (1964, page 431) state that the temperature factor for $T_1(0)$ is approximately twice that for the other T sites.

factor is much larger for $T_1(0)$ than for the other T atoms when an average scattering curve for $(\frac{1}{4}Al+\frac{3}{4}Si)$ is allocated to all T atoms in the structure.

(ii) *The* Na *atom*

Details of the environment of the (single) Na atom and of the half-atoms $Na_1$ and $Na_2$ of the split-atom model are given in Table 8, and thermal parameters in Table 4. Fig. 2 shows that the sodium atom is enclosed in a somewhat irregular oxygen-walled cavity. In the single-anisotropic-atom model, it has 5 neighbours at distances of less than 2·7 Å, forming a trigonal bipyramid, with 2 additional neighbours at distances less than 3 Å and a further 4 at distances less than 4 Å. This environment, though irregular, is of a type not unusual for sodium. If we adopt the split-atom model, the 'bonds' between $Na_1$ or $Na_2$ and O shown in Table 8 only have meaning in so far as it is permissible to ignore the small changes which are certain to occur in the positions of the oxygen atoms which form a cavity wall, according as one or other of these sodium atom sites is actually occupied within that cavity. (See also Jones & Taylor, 1968)

It must be emphasized that the use of the split-atom model to represent the highly anisotropic sodium atom in the course of the structure refinement is a purely geometrical device; it remains to consider whether it is possible to assign a unique physical interpretation to the observed anisotropy.

(*a*) In principle, the electron density distribution for the space average of a pair of atoms in sites with a small separation is different from the time average of a single atom performing anisotropic vibrations. In practice, for the degree of anisotropy (or split-atom separation) in low albite, the resolution achieved in the determination of electron density distribution is insufficient to distinguish between these two possible interpretations. This can be seen from the Appendix where it is shown that the half-separation of 0·18 Å in low albite is close to the limit below which no significant differences are to be expected under the existing experimental conditions.

(*b*) At a sufficiently low temperature the anisotropy should diminish if it represents true anisotropic thermal vibration, but not if it represents a space average. Williams (1961) showed that at −180 °C the anisotropy remains qualitatively unchanged from its magnitude at room temperature, but Williams & Megaw (1964) pointed out that while the most direct interpretation of this observation is in terms of a space average, the observation is not, in fact, incompatible with the alternative explanation in terms of thermal vibration. For in such a complex structure it is unlikely that the temperature dependence of the thermal vibration is controlled by the simple Debye relationship applicable when all interatomic forces are at least roughly comparable.

The conclusion reached is that it is not possible, on the structural evidence available, to decide whether the anisotropy of the sodium atom represents anisotropic thermal vibration or a space average; with due caution, it is permissible to say only that the low temperature measurements have their most obvious explanation in terms of space average.

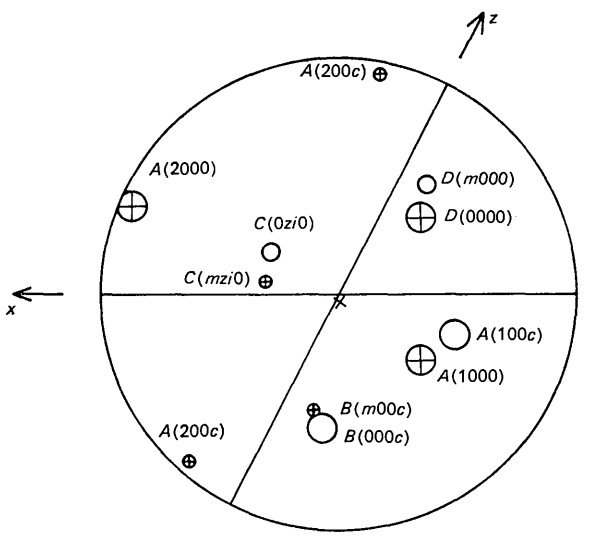


Fig. 2. Low albite. Stereogram of the environment of Na(0000), with (010) as plane of projection. Directions of $+x$ and $+z$ axes are shown; projection of $+y$ axis at × (in upper hemisphere). Oxygen atoms at less than 2·7 Å shown by large circles, between 2·9 Å and 3·0 Å by medium circles, between 3·2 Å and 4·0 Å by small circles; those in the upper hemisphere are crossed circles, those in lower hemisphere open circles.

(iii) *Structural models corresponding to a space average*

If it is assumed that the sodium atom anisotropy represents a space average, the simplest model is one in which, in different unit cells throughout the structure, the Na atom occupies one of two or more sites at random. Since, however, there is no physical reason why the sites should be of equal energy, the numbers occupying each site need not be equal. If there were only two possible sites, a very unsymmetrical electron-density peak might result. However, in this model small changes in the arrangement of the O atoms forming the cavity wall (according to the Na site occupied) are highly probable; this in turn implies that there will be associated *small* displacements or reorientations of the tetrahedron groups as a whole. These would tend to equalize the energies associated with the Na sites, but in so doing would modify their positions, so that ultimately we should expect a continuous distribution of sites.

An alternative interpretation is in terms of a perfectly regular alternation of $Na_1$ and $Na_2$ site occupation in a doubled unit cell in which the consequent small changes in O and T atom positions also show regular alternation. Since, however, the difference reflexions corresponding to the doubled repeat periodicity do not appear in the X-ray diffraction pattern, it

must further be assumed that there is a domain texture, small domains within which alternation is perfect being separated by fault boundaries across which there is a translation equal to the single cell periodicity. For example, if the doubled cell has $c=14$ Å instead of the observed albite 7 Å $c$ axis, the faulting displacement is 7 Å in the **c** direction. In such a faulted structure, only those reflexions corresponding to the sub-cell ($c\simeq 7$ Å) are observed; the structure deduced from them is in fact the average resulting from the superposition of the two sub-cells which constitute the true cell, and will show the split-atom $Na_1Na_2$ representation of anisotropy and the associated much smaller T and O atom anisotropies. For fuller discussion of these models, see Megaw (1959 and 1962) and Williams & Megaw (1964).

The doubled-cell structure is not favoured, by comparison with the random space average, except by arguments of a very general character – for example, multiple-cell structures with fault domains are known to occur in bytownite and in the intermediate plagioclases; and a doubled-cell structure may be more stable than a single-cell structure since the same total strains are distributed over twice the volume.

The general conclusion is, therefore, that a perfect structure with anisotropic thermal vibrations can account easily for all the observed effects except the low-temperature measurements already described, for which the arguments are inconclusive. In these circumstances considerable importance attaches to the nuclear magnetic resonance studies of Laves & Hafner (1962), which favour the time-average interpretation of the Na-atom anisotropy. If the low-temperature evidence is taken to rule out a thermal origin for the anisotropy, then a doubled-cell structure with fault domains is perhaps to be preferred to a random space average. In connexion with the time-average hypothesis the discussion of the anisotropy of the K atom in Pellotsalo microcline (Brown & Bailey, 1964) is of interest, though the anisotropy of the Na atom in low albite is very much more pronounced.

## 4. Refinement of the high albite structure

Intensity measurements for a complete three-dimensional refinement were made (by R. J. Traill) at the time of the two-dimensional study of high albite (Ferguson *et al.* 1958). These were converted to $F(hkl)$ values, all the usual corrections and correlations being applied, and provided 1797 observed $F$ values for the refinement of the structure.

The material used was an inverted Amelia (low) albite, prepared by heating for 16 days at 1065°C.

As with low albite, early stages in the refinement used the difference-Fourier program with the computer EDSAC II in Cambridge, later stages a least-squares program in Chicago. For the difference-Fourier pro-

Table 11. *High albite.*

(*a*) Final atomic coordinates, in fractions of cell edge.

| | $x$ | $y$ | $z$ |
|---|---|---|---|
| Na | 0·2743 | 0·0076 | 0·1320 |
| $T_1(0)$ | 0·0090 | 0·1652 | 0·2154 |
| $T_1(m)$ | 0·0048 | 0·8146 | 0·2288 |
| $T_2(0)$ | 0·6908 | 0·1083 | 0·3208 |
| $T_2(m)$ | 0·6854 | 0·8776 | 0·3533 |
| $O_A(1)$ | 0·0057 | 0·1349 | 0·9851 |
| $O_A(2)$ | 0·5923 | 0·9910 | 0·2781 |
| $O_B(0)$ | 0·8213 | 0·1091 | 0·2002 |
| $O_B(m)$ | 0·8187 | 0·8477 | 0·2456 |
| $O_C(0)$ | 0·0158 | 0·2906 | 0·2765 |
| $O_C(m)$ | 0·0217 | 0·6870 | 0·2191 |
| $O_D(0)$ | 0·1957 | 0·1123 | 0·3877 |
| $O_D(m)$ | 0·1884 | 0·8679 | 0·4260 |

(*b*) Split-atom coordinates of Na.

| Representation | $x$ | $y$ | $z$ | Isotropic temperature factors | Separation of split atoms |
|---|---|---|---|---|---|
| Na | 0·2743 | 0·0076 | 0·1320 | 5·7 Å² | — |
| $Na_1$ | 0·2698 | 0·9916 | 0·1567 | 2·1 | 0·61 Å |
| $Na_2$ | 0·2783 | 0·0260 | 0·1062 | 1·9 | |
| $Na_{1a}$ | 0·2661 | 0·0019 | 0·1516 | 1·7 | 0·41 |
| $Na_{1b}$ | 0·2756 | 0·9730 | 0·1766 | | |
| $Na_{2a}$ | 0·2826 | 0·0372 | 0·0928 | | 0·38 |
| $Na_{2b}$ | 0·2762 | 0·0126 | 0·1154 | | 0·90 (extreme separation) |

*Notes*: (1) Single atom model: Final atomic coordinates at end of stage (iv) of refinement. Anisotropic temperature factors, see Table 13. (2) Half-atom model: Isotropic temperature factors and coordinates at end of stage (ii) of refinement. Major axis of corresponding vibration ellipsoid is $B_{max}$. 9·4 Å², inclined at angles 67°, 41°, 133° to crystal axes $a$, $b$, $c$ (*cf.* Table 13, direction of principal vibration axis 73°, 41°, 128°). (3) Quarter-atom model: Isotropic temperature factor 1·7 Å² arbitrarily assigned. Atomic coordinates obtained at end of attempted quarter-atom refinement (*all* atoms) – see text, §5(iii).

gram the scattering factors were obtained by the method of Forsyth & Wells (1959), using the constants of Table 1, assuming full ionization, and allocating an average scattering factor ($\frac{1}{4}$Al+$\frac{3}{4}$Si) to all T atoms. For the least-squares program half-ionization was assumed, as for low albite, and the weighted average over both atoms again taken. Final coordinates are given in Table 11(*a*) and their errors in table 12.

(i) Starting with the atomic positions given by Williams (1961) for a synthetic high albite measured at −180 °C, (which include half-atoms $Na_1$ and $Na_2$ to represent the highly elongated Na atom) and with isotropic temperature factors $B_{1/2Na}$ 1·7 Å², $B_T$ 0·6 Å², $B_O$ 1·2 Å², 13 cycles of refinement of atomic coordinates reduced the *R*-index from 0·161 to 0·122. At the end of this stage a three-dimensional difference Fourier map showed that the half-atom representation of the Na atom was inadequate, that it would be necessary to assign individual isotropic temperature factors to all T and O atoms, and that most of these atomic peaks were unusually diffuse and so would probably need to be interpreted in terms of an average structure.

(ii) A further 10 cycles of refinement of both atomic coordinates and individual (isotropic) temperature factors for all atoms T, O, $Na_1$, $Na_2$, reduced *R* from 0·122 to 0·116. A quarter-atom model was examined; this is considered below [§§ 5(ii) (iii) and Table 11(*b*)].

(iii) For the first stage with the least-squares program the half-atoms $Na_1$ and $Na_2$ were replaced by a single (isotropic) Na atom, and 2 cycles of refinement of atomic coordinates and individual isotropic temperature factors resulted in an *R* index 0·120. This is larger than the *R* index (0·116) at the end of stage (ii) because the half-atom representation of Na used in stage (ii), though imperfect, is better than the single (isotropic) atom representation in stage (iii). The much larger (isotropic) temperature factors found for all atoms in stage (iii) (see Table 13) are a consequence of the different methods of refinement used in stages (ii) and (iii). For in stage (ii) the computer program selects *B* values to make the difference density ($\varrho_o-\varrho_c$) vanish *at* the atomic site, while in stage (iii) the program minimizes ($\varrho_o-\varrho_c$) in the environment of the atom. Fig. 3 illustrates this point by means of difference

Table 12. *High albite. Average coordinate errors*

| | Average error in coordinates* | | | Maximum error in position† |
|---|---|---|---|---|
| | $\sigma(x)$ | $\sigma(y)$ | $\sigma(z)$ | |
| Na | 0·0005 | 0·0005 | 0·0008 | 0·0064 Å |
| T | 0·0002 | 0·0001 | 0·0002 | 0·0016 |
| O | 0·0007 | 0·0003 | 0·0007 | 0·0057 |

* For atoms T and O the error quoted is the *average* for each coordinate.
† Error in atomic position is the maximum value $\sigma(x)a$, $\sigma(y)b$ or $\sigma(z)c$.

Table 13. *High albite. Thermal parameters*

| | Isotropic temperature factors (Å²) | | Anisotropic thermal parameters (Stage iv)† | | | | | | | | |
|---|---|---|---|---|---|---|---|---|---|---|---|
| | Stage (ii)* | Stage (iii)† | $b_{11}$ | $b_{22}$ | $b_{33}$ | $b_{12}$ | $b_{13}$ | $b_{23}$ | $B_{max}$ | $B_{int}$ | $B_{min}$ |
| | | | ($\times 10^{-4}$) | | | | | | (Å²) | | |
| Na | (1) 2·1<br>(2) 1·9 | 5·70 | 82 | 164 | 403 | 19 | 4 | −188 | 15·4 | 3·8 | 1·8 |
| $T_1(0)$ | 0·6 | 1·00 | 52 | 14 | 68 | −2 | 27 | 0 | 1·2 | 1·1 | 0·9 |
| $T_1(m)$ | 0·7 | 1·06 | 56 | 16 | 61 | 6 | 22 | 3 | 1·4 | 1·0 | 0·9 |
| $T_2(0)$ | 0·7 | 1·03 | 5 | 13 | 74 | 3 | 26 | 3 | 1·2 | 1·1 | 0·8 |
| $T_2(m)$ | 0·6 | 1·00 | 50 | 14 | 72 | 5 | 27 | 4 | 1·2 | 1·2 | 0·8 |
| $O_A(1)$ | 1·4 | 1·90 | 128 | 26 | 111 | 3 | 67 | −3 | 2·7 | 1·9 | 1·3 |
| $O_A(2)$ | 1·0 | 1·63 | 89 | 16 | 106 | 2 | 23 | 4 | 2·5 | 1·5 | 1·1 |
| $O_B(0)$ | 1·3 | 1·86 | 83 | 27 | 145 | −2 | 67 | −7 | 2·5 | 1·7 | 1·3 |
| $O_B(m)$ | 1·6 | 2·34 | 99 | 31 | 192 | 10 | 83 | −4 | 3·2 | 2·3 | 1·3 |
| $O_C(0)$ | 1·2 | 1·81 | 86 | 26 | 125 | −2 | 46 | 3 | 2·0 | 1·9 | 1·6 |
| $O_C(m)$ | 1·2 | 1·75 | 80 | 23 | 111 | 1 | 24 | −1 | 2·4 | 1·6 | 1·4 |
| $O_D(0)$ | 1·2 | 1·75 | 93 | 26 | 92 | 10 | 29 | 9 | 2·4 | 1·8 | 1·3 |
| $O_D(m)$ | 1·2 | 1·83 | 77 | 26 | 106 | 0 | 19 | 3 | 2·4 | 1·7 | 1·4 |

* Average *f* curve for fully ionized T atoms; $Na_1$–$Na_2$ separation 0·61 Å, for atomic coordinates quoted in Table 11(*b*).
† Average *f* curve for half-ionized T atoms.
Standard errors: for isotropic temperature factors Na 0·16, T 0·04, O 0·11 Å²; for anisotropic thermal parameters *b* Na 8, T 2, O 6 ($\times 10^{-4}$).
Anisotropic 'temperature factors' $B_{max}B_{int}B_{min}$ (along axes $r_3r_2r_1$) correspond to the anisotropic thermal parameters $b_{11}\ldots b_{23}$ for each atom.
For the Na atom the 'temperature factors' correspond to a 'vibration' ellipsoid with r.m.s. components of 'thermal' displacement 0·442, 0·219, 0·123 Å (average error 0·009 Å); the major axis is inclined at angles 73°, 41°, 128°, (average error 1°) to the crystallographic axes *a*, *b*, *c*.
[Further details of the orientations of the ellipsoids may be obtained on application to P. H. Ribbe.]

Fourier sections parallel to (100) through the T atoms at the end of stage (ii) and the end of stage (iii).

The resemblance of the directions of the T-atom anisotropies at stage (iii) to each other and to those of low albite at a comparable stage (see § 2, above, last paragraph) is rather striking, suggesting interaction with the Na anisotropy; it reinforces the need for caution in accepting these anisotropies as physically real.

(iv) In this final stage the single Na atom was retained but individual anisotropic temperature factors and atomic coordinates were refined, $R$ being reduced in 5 cycles from 0·120 to 0·082. As would be expected, most of this improvement in $R$ is the result of introducing anisotropic temperature factors for all atoms, the atomic coordinates being changed only slightly from those at the end of stage (ii).

This structure analysis supersedes that of Ferguson *et al.* (1958) and is effectively pressed as far as that of low albite (§ 2) for which the final $R$ index (0·068) was considerably lower. The difference is due to the much greater 'anisotropy' of the Na atom, and the greater diffuseness of the electron density distributions at T and O sites, in high albite; these features, characteristic of an 'average' structure, are discussed below. Details of atomic coordinates and their errors, thermal parameters, interatomic distances and interbond angles in the structure are given in Tables 11 to 17. The following points should be kept in mind in considering the interpretation of the tabulated information:

(*a*) The single sets of atomic positions and anisotropic thermal parameters of Tables 11(*a*) and 13 were derived [stage (iv) of the refinement] by the method of least squares, which does not reveal that the structure is an 'average'. This interpretation rests rather on the evidence of the difference-Fourier maps which show abnormally diffuse atoms, supported by comparison of the larger isotropic temperature factors assigned to atoms in high albite with those for low albite, at stages in the refinement when atomic positions have already

Table 14. *High albite.* T–O *bond lengths* (Å)

| | | Mean | | | Mean |
|---|---|---|---|---|---|
| $T_1(0)$ –$O_A(1)$ | 1·649 | | $T_2(0)$ –$O_A(2)$ | 1·654 | |
| –$O_B(0)$ | 1·645 | 1·648 | –$O_B(0)$ | 1·636 | 1·639 |
| –$O_C(0)$ | 1·642 | | –$O_C(m)$ | 1·633 | |
| –$O_D(0)$ | 1·654 | | –$O_D(m)$ | 1·632 | |
| $T_1(m)$–$O_A(1)$ | 1·656 | | $T_2(m)$–$O_A(2)$ | 1·655 | |
| –$O_B(m)$ | 1·629 | 1·644 | –$O_B(m)$ | 1·619 | 1·643 |
| –$O_C(m)$ | 1·650 | | –$O_C(0)$ | 1·646 | |
| –$O_D(m)$ | 1·641 | | –$O_D(0)$ | 1·653 | |

Average standard error in T–O bond lengths is $0{\cdot}005_9$ Å.
Standard error in mean T–O bond lengths is $0{\cdot}003_0$ Å.

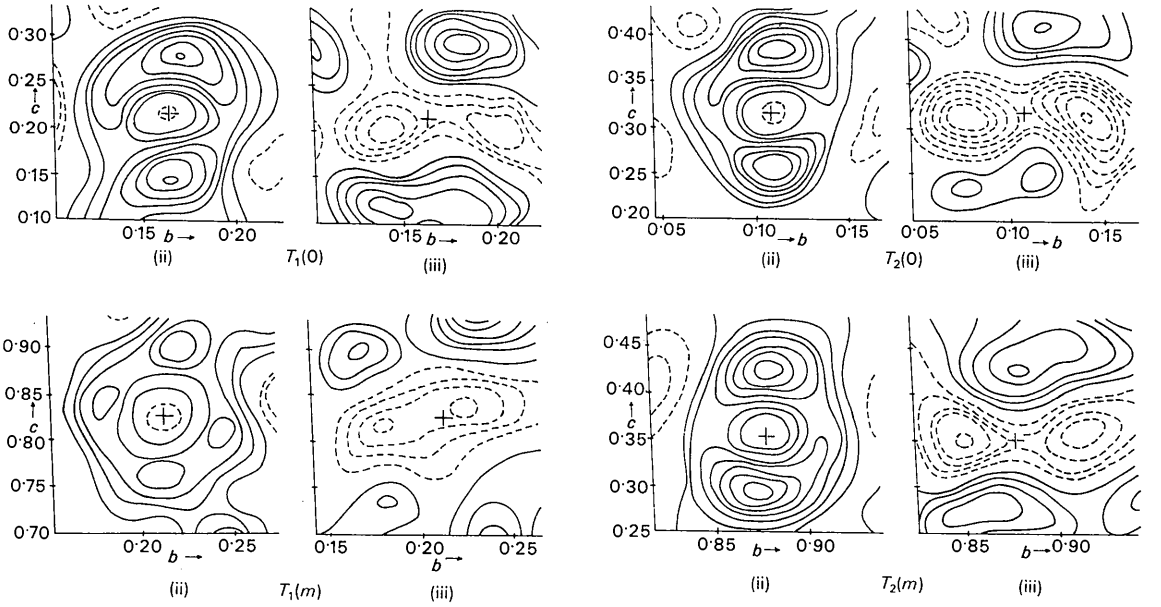


Fig. 3. High albite. Difference sections ($\varrho_o - \varrho_c$) parallel to (100) through the centres of the tetrahedral atoms Al, Si. The atomic site is marked by a cross; positive contours full line, negative dotted, zero contour omitted; contour interval 0·165 e.Å$^{-3}$. For each atom, section on left corresponds to stage (ii) of refinement, when ($\varrho_o - \varrho_c$) is minimized at the atomic site; section on right to stage (iii), when ($\varrho_o - \varrho_c$) is minimized in the neighbourhood of the atom.

Table 15. *High albite.* O–O *interatomic distances* (Å)

| Tetrahedron | $O_A$–$O_B$ | $O_A$–$O_C$ | $O_A$–$O_D$ | $O_B$–$O_C$ | $O_B$–$O_D$ | $O_C$–$O_D$ | Tetrahedral mean |
|---|---|---|---|---|---|---|---|
| $T_1(0)$ | 2·606 | 2·771 | 2·616 | 2·706 | 2·734 | 2·696 | 2·688 |
| $T_1(m)$ | 2·627 | 2·743 | 2·632 | 2·705 | 2·705 | 2·689 | 2·684 |
| $T_2(0)$ | 2·663 | 2·609 | 2·666 | 2·699 | 2·691 | 2·718 | 2·674 |
| $T_2(m)$ | 2·688 | 2·651 | 2·675 | 2·676 | 2·680 | 2·726 | 2·683 |
| Bond mean | 2·646 | 2·693 | 2·647 | 2·697 | 2·703 | 2·707 | |

Average standard error in O–O bond lengths is $0{\cdot}008_1$ Å.
Standard error in tetrahedral mean bond lengths is $0{\cdot}003_3$.

Table 16. *High albite. Interbond angles, in degrees*

| T–O–T angles | | O–T–O angles | | | | | |
|---|---|---|---|---|---|---|---|
| $T_1(0)$ –$O_A(1)$ –$T_1(m)$ | 143·1 | $O_A(1)$–$T_1(0)$ | –$O_B(0)$ | 104·6 | $O_A(2)$–$T_2(0)$ | –$O_B(0)$ | 108·1 |
| $T_2(0)$ –$O_A(2)$ –$T_2(m)$ | 129·7 | | –$O_C(0)$ | 114·7 | | –$O_C(m)$ | 105·1 |
| $T_1(0)$ –$O_B(0)$ –$T_2(0)$ | 141·5 | | –$O_D(0)$ | 104·8 | | –$O_D(m)$ | 108·5 |
| $T_1(m)$–$O_B(m)$–$T_2(m)$ | 158·7 | $O_B(0)$– | –$O_C(0)$ | 110·8 | $O_B(0)$– | –$O_C(m)$ | 111·3 |
| $T_1(0)$ –$O_C(0)$ –$T_2(m)$ | 130·5 | | –$O_D(0)$ | 112·0 | | –$O_D(m)$ | 110·9 |
| $T_1(m)$–$O_C(m)$–$T_2(0)$ | 134·3 | $O_C(0)$– | –$O_D(0)$ | 109·8 | $O_C(m)$– | –$O_D(m)$ | 112·7 |
| $T_1(m)$–$O_D(0)$ –$T_2(m)$ | 135·2 | | | | | | |
| $T_1(m)$–$O_D(m)$–$T_2(0)$ | 149·1 | $O_A(1)$–$T_1(m)$–$O_B(m)$ | | 106·2 | $O_A(2)$–$T_2(m)$–$O_B(m)$ | | 110·4 |
| | | | –$O_C(m)$ | 112·2 | | –$O_C(0)$ | 106·9 |
| Mean | 140·3 | | –$O_D(m)$ | 106·0 | | –$O_D(0)$ | 107·9 |
| | | $O_B(m)$– | –$O_C(m)$ | 111·2 | $O_B(m)$– | –$O_C(0)$ | 110·1 |
| | | | –$O_D(m)$ | 111·6 | | –$O_D(0)$ | 110·0 |
| | | $O_C(m)$– | –$O_D(m)$ | 109·6 | $O_C(0)$– | –$O_D(0)$ | 111·5 |

Mean tetrahedral angle 109·45°

Standard error of all bond angles is 0·2°.

been determined with considerable accuracy. Similarly, the anisotropic thermal parameters of the final structures are larger for high albite than for low.

(*b*) In Table 17 the Na–O interatomic distances correspond to the final atomic coordinates of Table 11(*a*), whereas the distances for $Na_1$–O and $Na_2$–O (half-atom model) are calculated from the $Na_1$, $Na_2$ coordinates listed in Table 11(*b*) and the O coordinates (*not* listed) at the same stage (ii) of the refinement process. Comparison may be made with low albite, Table 8, where the situation is similar, and where in particular the O atom coordinates also differ very little from the final values.

Table 17. *High albite.* Na–O *interatomic distances* (Å)

| Oxygen | Na(0000) | $Na_1$(half-atom) | $Na_2$(half-atom) |
|---|---|---|---|
| $O_A$(1000) | 2·60 | 2·54 | 2·48 |
| $O_A$(100*c*) | 2·71 | 2·74 | 2·92 |
| $O_A$(2000) | 2·34 | 2·37 | 2·34 |
| $O_A$(200*c*) | 3·53 | | 3·33 |
| $O_A$(200*c*) | 3·84 | | |
| $O_B$(000*c*) | 2·53 | 2·57 | 2·53 |
| $O_B$(*m*00*c*) | 3·17 | 3·45 | 2·88 |
| $O_C$(0*zi*0) | 3·37 | 3·20 | 3·57 |
| $O_C$(*mzi*0) | 2·91 | 3·12 | 2·68 |
| $O_D$(0000) | 2·51 | 2·46 | 2·58 |
| $O_D$(*m*000) | 3·13 | 2·84 | 3·44 |

Distances Na–O are calculated from the final atomic coordinates of Table 11(*a*). The atomic coordinates of the half-atoms $Na_1$ and $Na_2$ are quoted in Table 11(*b*). For other atomic coordinates, see text.

Average standard error in Na–O bond lengths is $0{\cdot}008_6$ Å.

## 5. Discussion of the high albite structure

The average high albite structure is first discussed in relation to the Al,Si distribution and the environment and anisotropy of the Na atom. Evidence bearing on the interpretation of the average structure in terms of a faulted domain model is then reviewed.

### (i) *The* Al,Si *distribution*

The mean tetrahedron sizes and corresponding Al contents show no statistically significant departure from the completely random distribution with 0·25 Al in each T site (Table 18). It is, however, interesting to note that the tetrahedron $T_1(0)$, as measured, is slightly larger than the others, as would be expected if inversion from the original low temperature form were not quite complete; a similar effect is seen in the measurements of Ferguson *et al.* (1958), included in Table 18 for comparison. Alternatively, it could be explained as a local (but periodic) strain of the framework, due to the topology of the structure.

Temperature factors derived in the course of the refinement of the structure depend upon the refinement procedure used and assumptions made (for example: about the state of ionization of the atom). It is, however, interesting to note that the isotropic temperature factors for atoms T (0·6 Å$^2$) and O (1·2 Å$^2$) in sanidinized orthoclase with random Al,Si distribution (Ribbe 1963) are very similar to those of high albite determined by the same difference-Fourier refinement program with the same assumed scattering powers.

(ii) *The* Na *atom: anisotropy and environment*

The elongated cavity within which the Na atom is enclosed is formed by the same group of eleven O atoms, at distances less than 4 Å, as in low albite. The most noticeable difference, in the single-atom model, is the change in the relative distances to the two $O_C$ neighbours 0*zi*0 and *mzi*0. For such extreme anisotropy as is shown in Table 13, the relative 'bond lengths' will of course be very sensitive to differences in the models used for the Na positions. Values calculated for the half-atom model in Table 17 are not necessarily good approximations to those for the quarter-atom model, but are included to show the order of magnitude of the differences to be expected. For example, the apparent near equality of the distances to $O_B$(*m*00*c*) and $O_D$ (*m*000) in the single-atom model (in contrast to their marked inequality in low albite) is, in the other models, the consequence of averaging. Moreover, in the split-atom models, where the anisotropy is so large, it is unrealistic to ignore changes in the cavity walls with changes in the sites occupied, and hence of doubtful value to use the term 'bond' for the contacts of Table 17.

As with low albite, the use of a split-atom representation of the Na-atom anisotropy is for convenience in the first instance, and does not of itself imply that a space average is favoured in comparison with a time average (*i.e.* a true anisotropic thermal vibration).

The split-atom model which best fits the observations has the four quarter-atoms nearly collinear and symmetrical about their mean position, the outer pair with a separation of ~0·9 Å, the inner ~0·2 Å. This arrangement resembles the hypothetical model of the Appendix (where, however, the separation of the inner pair is zero) closely enough to allow comparison. The conclusion reached from the hypothetical model agrees with that from the structure analysis, namely that with this anisotropy and this use of the diffraction evidence, a clear distinction cannot be made between a quarter-atom model and an anisotropic-atom model, but that a half-atom model would be distinguishable.

It is found that the best half-atom model (*cf.* Tables 11(*b*) and 17, separation 0·61 Å) is not satisfactory in representing the observed electron density distribution for the Na atom. Fig. 4(*a*) is a difference density section through the single Na atom, corresponding to the atomic coordinates of Table 11(*a*) and an isotropic temperature factor *B* 5·7 Å$^2$. Fig. 4(*b*), the corresponding section through $Na_1$, $Na_2$, is obviously much less satisfactory than the corresponding Fig. 1(*b*) for low albite; to achieve comparably close representation, the quarter-atom model of Fig. 4(*c*) and Table 11(*b*) is required.

There are, however, other lines of argument suggesting that the quarter-atom model is correct. Firstly, it seems very unrealistic to suppose that the Na atom would vibrate within its cavity with amplitude corresponding to the displacements quoted in Table 13. Secondly, the observation* (Williams 1961; Williams & Megaw, 1964) that the anisotropy is effectively unchanged at −180 °C is easier to explain if this effect is a space average rather than a time average. Thirdly, quarter-atom splitting of the Na atom, if it represented ordered occupation of sites in a quadripartite cell rather than a random space average, would imply quarter-atom splitting of T atoms and O atoms, not necessarily collinear like the Na splitting; there was some indication of this at the end of stage (ii) of the refinement process, and a few cycles of subsequent refinement with this hypothesis caused the *R*-value to fall from 0·116 to 0·106. Fourthly, the quarter-atom splitting of Na is closely related to the observed structure of other felspars, as discussed in more detail below. Against this must be set the fact that the splittings of T and O atoms, at the stage reached when the refinement of the quarter-atom model was discontinued, could not be clearly related to effects in other felspars.

(iii) *Model assuming a multipartite unit cell and fault domains*

In the case of low albite it was possible to offer only an extremely tentative suggestion that the structure determined from the diffraction pattern might represent a space average and, if so, that this could arise from the occurrence of faulting in a structure with bipartite or multipartite cells. For high albite, as we have seen above, the evidence for an average structure is much stronger. Similarly, its interpretation in terms of a structure with multipartite cells is much more readily acceptable on the basis of a prediction of the probable existence of such a structure by Megaw (1959) and her later development of the concept (Me-

* Although Williams studied a synthetic high albite, not necessarily structurally identical with the inverted Amelia albite of this paper (Ferguson *et al.*, 1958), it seems reasonable to suppose that his findings are applicable here.

Table 18. *High albite.* Al, Si *distribution*

| | (1) This investigation | | (2) Ferguson *et al.* (1958) | |
|---|---|---|---|---|
| Tetrahedron | Mean T–O distance | Al content | Mean T–O distance | Al content |
| $T_1(0)$ | 1·648 Å | 0·27 | 1·652 Å | 0·30 |
| $T_1(m)$ | 1·644 | 0·24 | 1·639 | 0·21 |
| $T_2(0)$ | 1·639 | 0·21 | 1·642 | 0·23 |
| $T_2(m)$ | 1·643 | 0·24 | 1·647 | 0·26 |
| | | 0·96 | | 1·00 |

*Note*: Al contents are deduced in *both* cases from the relationship of Smith & Bailey (1963). See also Ribbe & Gibbs (1967), Jones (1968).

gaw, 1962; see also Williams & Megaw, 1964). The central feature of the quadripartite cell model is that there is a close relationship linking all high plagioclases – even high albite at the Na-rich end of the series – with the anorthite structure; this relationship rests on the consideration of cell dimensions, Al,Si distribution, and cation environments. The application of statistical tests (Ribbe, 1963; Srinivasan & Ribbe, 1965; Fleet, Chandrasekhar & Megaw, 1966) provided supporting evidence for a close relationship between high albite and the anorthite structures, and so for the validity of Megaw's model. If the model is indeed applicable to high albite, then the average structure represents the superposition of the four slightly different subcells which comprise the true unit cell of the structure manifested within a single domain; adjacent domains are separated by out-of-step boundaries so that no difference reflexions are observed. Each atom of the average structure should therefore show quarter-atom splittings in a map of the electron density distribution of sufficient resolution. Any marked resemblance between the split-atom map of albite and a map of the average structure of anorthite or bytownite (Fleet, 1961; Fleet, Chandrasekhar & Megaw, 1966) constructed by superimposing their albite-like subcells is therefore evidence for the existence of a multipartite true cell in albite. Though resemblance of the T and O atom splittings had not been found when quarter-atom refinement was discontinued, the quarter Na atoms have positions falling neatly into place in a single curve covering the high plagioclases for which the structure is known (Megaw, unpublished). A fuller discussion of the quarter-atom model awaits the completion of a three-dimensional refinement of the andesine structure now in progress in this laboratory.

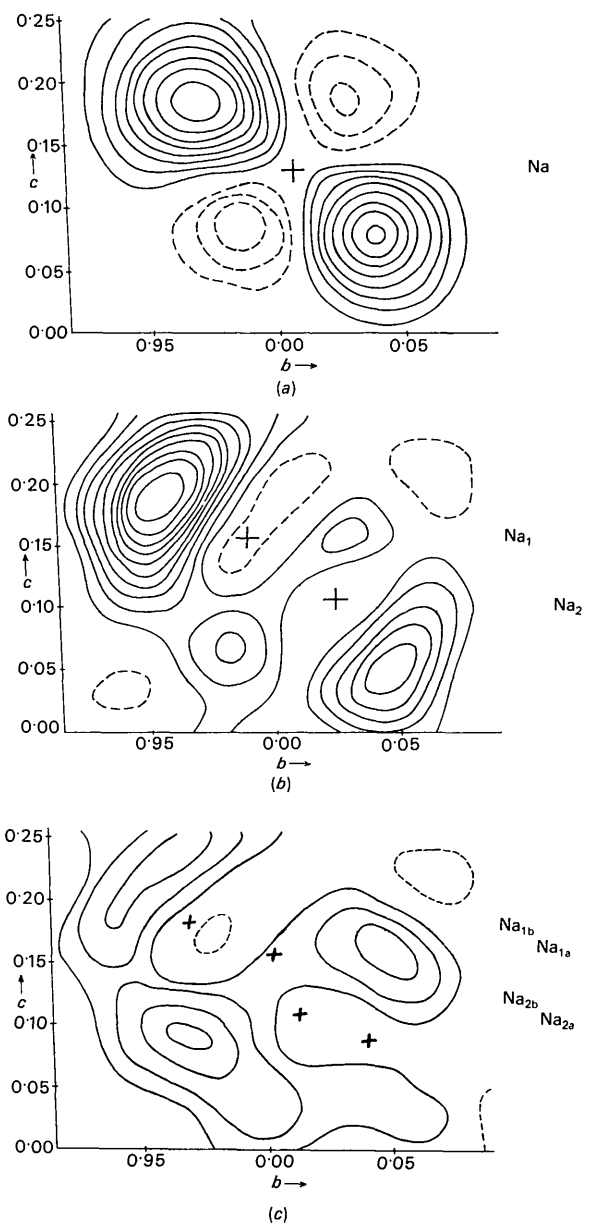


Fig. 4. High albite. The anisotropy of the sodium atom shown in difference sections ($\varrho_o - \varrho_c$) parallel to (100) and passing through the centre of the atom Na and near the centres of the half-atoms and quarter-atoms of Table 11(*b*). Positive contours full line, negative dotted, zero contour omitted. Contour interval 0·165 e.Å$^{-3}$.

In summary, therefore, a quadripartite model with a domain texture is definitely supported by the experimental evidence, but the resolution achieved in the analysis is not sufficient to establish unequivocally the structure within the domains.

## 6. Conclusion

The completion of the three-dimensional refinements, resulting in the determination of the average structures of low albite and high albite with considerable accuracy, marks the end of a well-defined stage in the study of sodium felspar. A number of questions remain unanswered, some of which have been mentioned in preceding sections.

The most obvious outstanding problem is whether the sodium atom anisotropy represents true thermal vibration, or a space average, and, if the latter, a random space average or a faulted domain average. A more detailed and accurate study, preferably at temperatures lower than the −180 °C used by Williams (1961), might permit a definite decision between thermal vibration and space average; if the anisotropy represents a space average, enhanced accuracy and resolution in a room-temperature study might, by breaking up the average peaks into sets of two or four peaks which can be allocated to different subcells, provide evidence for a multipartite structure as contrasted with a random space average. Either of these investigations represents a formidable undertaking. Grouping of intensities by shells in reciprocal space, or selection for detailed study of reflexions sensitive to the differences between the models, might give some help in either case.

More immediately feasible would be to examine whether it is correct to speak of 'the high albite structure', or whether several high albite structures exist, depending, for example, on the thermal history of the material. One source of confusion in such a study was removed by the work in this laboratory of Hall & Quareni (private communication, 1964; see also Hall & Quareni, 1967) when they demonstrated the non-existence of the monoclinic structure 'monalbite' reported by Brown (1960) as resulting from prolonged heating of triclinic high albite (see also Brown, 1967; Grundy, Brown & MacKenzie, 1967). This serves only to emphasize the need for the careful experimental study of such questions as whether for example there are significant differences between a synthetic high albite, produced directly, and a high albite (such as that studied here) produced by heating a material initially in the low-temperature form [see footnote to § 5(ii)].

Finally, the interesting relationships between high temperature plagioclases (including albite) and anorthite, to which reference has already been made in §5(iii), will repay further study as other structures (*e.g.* andesine) are refined to a comparable accuracy.

The authors' indebtedness to Professor R. B. Ferguson and Dr R. J. Traill, who kindly furnished their experimental measurements (partly processed for the refinement of the structures) is made clear in the heading to the text; thanks are also due to Professor Ferguson and Dr Traill, and to many other colleagues, for helpful comments during the preparation of the text.

The University Mathematical Laboratory, Cambridge, and the University of Chicago Computer Unit provided computing facilities and assistance with the lengthy refinement procedures; the authors are especially indebted to Professor M. V. Wilkes and Mrs J. C. Matthewman (Cambridge) and to Mr C. R. Knowles (Chicago).

One of us (P. H. R.) acknowledges the award of a Fulbright Studentship, during the tenure of which this work was done. The research forms a part of the laboratory's study of felspar structures under W. H. T. and H. D. M., a project supported by generous grants provided originally by the Department of Scientific and Industrial Research, now by the Natural Environment Research Council.

## APPENDIX

### Comparison of effects of temperature factor and 'splitting' of atoms

By Helen D. Megaw

In a disordered structure where two possible sites in the unit cell are occupied at random (or with only local order) the electron-density map shows a half atom at each possible site. If the sites are close together, the half atoms overlap and a single elongated peak results. We compare this with the effect of a single atom possessing an anisotropic temperature factor.

We use orthogonal axes of reference. Let the first model be a pair of half atoms at $(x \pm d/a, y, z)$, with an isotropic temperature factor $\exp\left[-\beta_0\left(\frac{h^2}{a^2}+\frac{k^2}{b^2}+\frac{l^2}{c^2}\right)\right]$, and let the second model be a single atom at $(x,y,z)$, with an anisotropic temperature factor

$$\exp\left[-(\beta_0+\beta_1)\frac{h^2}{a^2}-\beta_0\left(\frac{k^2}{b^2}+\frac{l^2}{c^2}\right)\right].$$

Their contributions to the structure factor $F(hkl)$ will be the same except that the first has a factor $\cos 2\pi hd/a$ where the second has a factor $\exp(-\beta_1 h^2/a^2)$. If the temperature factors are written in the form $\exp[-B(\sin\theta/\lambda)^2]$, $B_{\text{iso}}=B_{\min}=4\beta_0$, $B_{\max}=4(\beta_0+\beta_1)$; hence $\beta_1=\frac{1}{4}(B_{\max}-B_{\min})$.

Suppose that one model represents the true structure and the other model is assumed for purposes of calculation. Then the process of refinement involves matching the two functions as well as possible over the whole range of observational data, and the result can be expressed either in terms of $d$ or of $\beta_1$ (or $B_{\max}-B_{\min}$).

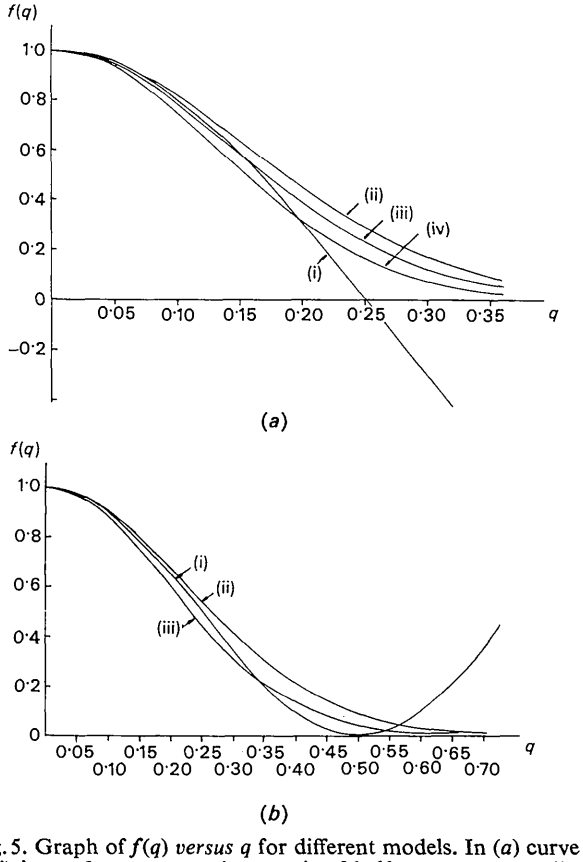


Fig. 5. Graph of $f(q)$ *versus* $q$ for different models. In (*a*) curve (i) is $\cos 2\pi q$, representing a pair of half atoms; curves (ii), (iii), (iv) are $\exp[-2\pi^2(kq)]$, representing an anisotropically vibrating atom, with adjustable constant $k=1{\cdot}0$, $1{\cdot}1$, $1{\cdot}2$ respectively. In (*b*) curve (i) is $\cos^2 \pi q$, representing the linear quarter-atom model described in the text; (ii) and (iii) are $\exp[-2\pi^2(kq)^2]$, with $k=0{\cdot}7$, $0{\cdot}8$ respectively.

It is convenient to work in terms of the reciprocal-space vector **S**, and to define a new variable $q=S_x d$, where $S_x=\mathbf{S}\,.\,\mathbf{a}/a$, $|S|=2\sin\theta/\lambda$. Thus $q$ is proportional to a reciprocal-space vector parallel to the direction of elongation, but its magnitude depends on the splitting. Since $2\pi hd/a=2\pi S_x d=2\pi q$, and $\beta_1 h^2/a^2=\beta_1 S_x^2=\beta_1 q^2/d^2$, the functions to be compared are $\cos 2\pi q$ and $\exp(-\beta_1 q^2/d^2)$. These coincide for small $q$ if

$$\tfrac{1}{2}(2\pi q)^2=\beta_1 q^2/d^2$$

*i.e.*

$$\beta_1=2\pi^2 d^2\,.$$

We wish to match the curves over the whole range, and therefore compare the functions $\cos 2\pi q$ and $\exp[-2\pi^2(kq)^2]$ where $k$ is a constant close to unity to be found empirically, and $\beta_1=2\pi^2 k^2 d^2$.

Fig. 5(*a*) shows $\cos 2\pi q$ [curve (i)] and the exponential function drawn for $k=1$, 1·1, 1·2 (curves (ii), (iii), (iv) respectively). The choice of $k$ depends on the maximum experimental value of $q$; if $q_m$ were about 0·19, (iii) would be a very good fit, while if $q_m$ were about 0·25, (iv) would be better. Bad misfits only set in above about $q_m=0{\cdot}25$.

We make the working assumption that it will be reasonable to use the two models interchangeably if $q_m<0{\cdot}25$, provided the intensities are not separated out in shells of different $S$ or $S_x$, but are all used together. Then we may calculate the corresponding values of $d$ and $\beta_1$ when the limit of observation is at $S_x=S_m$. We have

$$d_{lt}=0{\cdot}25/S_m$$

and

$$\beta_{lt}=2\pi^2 k^2 d_{lt}^2=2\pi^2(0{\cdot}30/S_m)^2$$

or

$$(B_{\max}-B_{\min})_{lt}=8\pi^2(0{\cdot}30/S_m)^2\,.$$

If the average atom is a complex of more than two split-atom peaks, it is harder to achieve resolution. Consider as illustration a quarter-atom model, with two quarter atoms at $(x,y,z)$, and two at $(x\pm d/a,y,z)$. The factor $\cos 2\pi q$ is now replaced by $\frac{1}{2}(1+\cos 2\pi q)$ or $\cos^2\pi q$, shown in Fig. 5(*b*), curve (i), which is matched very well by an exponential function out to $q=0{\cdot}60$; curves (ii) and (iii) have $k=0{\cdot}7$ and 0·8 respectively, but the fit is obviously not critical. Taking $k=0{\cdot}75$ we have, for this model

$$d_{lt}=0{\cdot}60/S_m$$

$$(B_{\max}-B_{\min})_{lt}=8\pi^2(0{\cdot}45/S_m)^2\,.$$

Applying these to the albites, we note that $S_m\simeq 1{\cdot}5$ Å$^{-1}$. For the half-atom model, this gives $d_{lt}=0{\cdot}17$ Å, $(B_{\max}-B_{\min})_{lt}=3{\cdot}2$ Å$^2$, which may be compared with the low albite results, $d=0{\cdot}18$ Å, $B_{\max}-B_{\text{int}}=4{\cdot}0$ Å$^2$. For the quarter-atom model, $d_{lt}=0{\cdot}40$ Å, $(B_{\max}-B_{\min})_{lt}=7{\cdot}2$ Å$^2$, which may be compared with the high albite results, $d_{\text{extreme}}=0{\cdot}45$ Å, $B_{\max}-B_{\text{int}}=11{\cdot}6$ Å$^2$. This suggests that low albite is close to the limit where the models with half-atom and anisotropic atoms are interchangeable, and high albite similarly close to the limit for a simple quarter-atom model.

Adoption of the wrong model, of course, introduces errors. The diagrams show that if $q_m$ is less than the specified limit $q_{lt}$ (0·25 or 0·60 in the two examples), the error in the contribution of the atom concerned is not likely to be more than 10% of the average contribution; the resulting percentage error in $F(hkl)$ will be rather less, and will therefore be comparable with the random error commonly found in visually estimated intensities. Since it is systematic its effects may not be completely negligible (unless we go to considerably lower values of $q$), but it will be hard to make use of it to discriminate between the models unless all other comparable systematic errors (*e.g.* absorption errors) have been eliminated. With $q_m$ close to or slightly above $q_{lt}$ we may therefore expect small systematic effects from the use of the wrong model, particularly on the anisotropies of the other atoms. With $q_m$ appreciably above $q_{lt}$ we may hope for resolution, especially if the intensity data are sorted out according to their $S_x$ values for analysis.

## References


Appleman, D. E. & Clark, J. R. (1965). *Amer. Min.* **50**, 1827.

Berghuis, J., Haanappel, IJ. M. ,Potters, M., Loopstra, B. O., MacGillavry, C. H. & Veenendaal, A. L. (1955). *Acta Cryst.* **8**, 478.

Brown, B. E. & Bailey, S. W. (1964). *Acta Cryst.* **17**, 1391.

Brown, W. L. (1960). *Z. Kristallogr.* **113**, 297.

Brown, W. L. (1967). *Miner. Mag.* **36**, 80.

Busing, W. R., Martin, K. O. & Levy, H. (1962). *ORFLS, A Fortran crystallographic least-squares program.* ORNL-TM-305, Oak Ridge National Laboratory, Tennessee.

Clark, J. R. & Appleman, D. E. (1960). *Science*, **132**, 1837.

Cruickshank, D. W. J. (1949). *Acta Cryst.* **2**, 65, 154.

Ferguson, R. B., Traill, R. J. & Taylor, W. H. (1958). *Acta Cryst.* **11**, 331.

Finney, J. J. & Bailey, S. W. (1964). *Z. Kristallogr.* **119**, 413.

Fleet, S. G. (1961). Thesis for Ph. D., Cambridge.

Fleet, S. G., Chandrasekhar, S. & Megaw, H. D. (1966). *Acta Cryst.* **21**, 782.

Forsyth, J. B. & Wells, M. (1959). *Acta Cryst.* **12**, 412.

Froese, C. (1957). *Proc. Camb. Phil. Soc.* **53**, 206.

Grundy, H. D., Brown, W. L. & MacKenzie, W. S. (1967). *Miner. Mag.* **36**, 83.

Hall, K. M. & Quareni, S. (1967). *Miner. Mag.* **36**, 78.

*International Tables for X-ray Crystallography* (1962). Vol. III. Birmingham: Kynoch Press.

Jones, J. B. (1968). *Acta Cryst.* B**24**, 355.

Jones, J. B. & Taylor, W. H. (1968). *Acta Cryst.* **B 24**, 1387.

Laves, F. & Hafner, S. (1962). *Norsk Geol. Tidsskr.* **42**(2), 57.

Megaw, H. D. (1959). *Miner. Mag.* **32**, 226.

Megaw, H. D. (1962). *Norsk Geol. Tidsskr.* **42**(2), 104.

Ribbe, P. H. (1963). Thesis for Ph.D., Cambridge.

RIBBE, P. H., FERGUSON, R. B. & TAYLOR, W. H. (1962). *Norsk Geol. Tidsskr.* **42**(2), 152.
RIBBE, P. H., FERGUSON, R. B., TRAILL, R. J. & TAYLOR, W. H. (1963). *Geol. Soc. Amer. Ann. Meetings*, New York, 136A.
RIBBE, P. H. & GIBBS, G. V. (1967). *Trans. Amer. Geophys. Union.* **48**, 230.
SMITH, J. V. (1954). *Acta Cryst.* **7**, 479.
SMITH, J. V. & BAILEY, S. W. (1963). *Acta Cryst.* **16**, 801.
SRINIVASAN, R. & RIBBE, P. H. (1965). *Z. Kristallogr.* **121**, 21.
TAYLOR, W. H., DARBYSHIRE, J. A. & STRUNZ, H. (1934). *Z. Kristallogr.* **87**, 464.
WILLIAMS, P. P. (1961). Thesis for Ph. D., Cambridge.
WILLIAMS, P. P. & MEGAW, H. D. (1964). *Acta Cryst.* **17**, 882.

*Acta Cryst.* (1969). B**25**, 1518

# The Crystal Structure of Bis(succinodinitrile)copper(I) Perchlorate

BY J. F. BLOUNT* AND H. C. FREEMAN
*School of Chemistry, University of Sydney, Sydney, Australia*

AND P. HEMMERICH† AND C. SIGWART‡
*Institute for Inorganic Chemistry, University of Basel, Basel, Switzerland*

(*Received* 8 *August* 1968)

Bis(succinonitrile)copper(I) perchlorate crystallizes in the space group $P4_2/nmc$ with two formula units $Cu(NCCH_2CH_2CN)_2ClO_4$ in a unit cell of dimensions $a=7{\cdot}68_0\pm0{\cdot}01$, $c=10{\cdot}18_8\pm0{\cdot}01_5$ Å ($D_m=1{\cdot}78\pm0{\cdot}01$ g.cm$^{-3}$, $D_c=1{\cdot}786$ g.cm$^{-3}$). 288 independent intensities above background were collected on a diffractometer by an $\omega$-scan technique. The structure was refined by full-matrix least squares to a conventional unweighted $R$ index of 3·8% for all data. The structure consists of infinite puckered sheets of composition $[Cu(NCCH_2CH_2CN)_2^+]_\infty$ normal to **c**, with $ClO_4^-$ ions lying in the planes of the sheets. The succinonitrile molecules are statistically disordered about the ⟨100⟩ mirror planes. Each Cu atom is tetrahedrally surrounded by four nitrogen atoms at a Cu–N distance of $1{\cdot}987\pm0{\cdot}005$ Å. Each succinonitrile is coordinated to two Cu atoms. The Cu–N≡C–C segment is nearly linear with a Cu–N–C angle of $169{\cdot}7\pm0{\cdot}5°$ and N–C–C angle of $178{\cdot}3\pm0{\cdot}4°$.

## Introduction

Among the rapidly growing number of precise crystal structure analyses of copper complexes, those dealing with Cu(I) complexes form a small minority compared with those in which the metal is Cu(II). This is unfortunate, since accurate and precise geometrical information concerning copper in both its oxidation states is essential, for instance, for an understanding of the redox behaviour of coordinated copper which, in turn, has important biological implications (Hemmerich, 1966; Freeman, 1966). The present study is a contribution to the stereochemistry of tetrahedral Cu(I).

## Experimental

$Cu(CH_3CN)_4ClO_4$ [2g, prepared by the method of Hemmerich & Sigwart (1963)] was dissolved under nitrogen in a solution of succinodinitrile§ (10 g) and absolute dimethylformamide (2 g). The mixture was heated to 140 °C for three hours, and was then allowed to cool to room temperature. $Cu(NCCH_2CH_2CN)_2ClO_4$ (1·35 g) was precipitated in the form of pale grey-brown crystals, approximately cubic in shape and detonating at 298 °C. Titration with $KMnO_4$ showed the molecular weight to be $323\pm6$ (calc. 323·2).

Neither visual nor X-ray examination showed any change in the crystals as a result of exposure to air, even after a period of weeks. The density was determined by the flotation method with mixed solvents, $BrCH_2CH_2BR$ and $CCl_4$. The space group was determined from *hk*0, *hk*1, *hk*2 and *hhl* precession photographs of a crystal mounted about its [110] axis. The lattice constants were fitted by least squares to $\sin^2\theta/\lambda^2$ for 24 reflexions ($12\alpha_1,\alpha_2$ pairs) measured on an 0*kl* Weissenberg photograph calibrated with Al powder lines ($a=4{\cdot}0489$ Å; Cu $K\alpha_1=1{\cdot}54051$ Å; $K\alpha_2=1{\cdot}54433$ Å). A variant of Cohen's analytical extrapola-

* Present address: Physical Chemistry Section, Hoffmann-La Roche, Inc., Nutley, New Jersey 07110, U.S.A.
† Present address: University of Konstanz, Konstanz, Germany.
‡ Present address: Department of Chemistry, Utah State University, Logan, Utah 84321, U.S.A.

§ 'Succinonitrile' is the common name of the compound more properly named 'succinodinitrile'. Herein we use the two terms interchangeably.